Acta Materialia 316 (2026) 122453

Contents lists available at ScienceDirect

Acta Materialia

journal homepage: www.elsevier.com/locate/actamat

Atomistic understanding of interdependence of crystal growth of two seeds embedded in glass

R. Thapa [a], H. Jain [a,*], V. Dierolf [b], M.E. McKenzie [c]

[a] Department of Materials Science and Engineering, Lehigh University, Bethlehem, PA 18015, USA
[b] Department of Physics, Lehigh University, Bethlehem, PA 18015, USA
[c] Corning Incorporated, Science and Technology Division, Corning, NY 14831, USA

ARTICLE INFO

Keywords:
Crystallization
Glass
Molecular dynamics

ABSTRACT

Recent results showed that during growth, a crystal seed embedded in glass experiences nonuniform forces from the host matrix. This result raised the possibility that during devitrification of glass, the growth of a crystal can be affected by the presence of neighboring crystals. To investigate the nature of any such interdependence of growth of neighboring crystals, atomic scale morphology of two seeds growing in a glass matrix was simulated as a function of their separation and relative misorientation. The results show a coupled rotation of seeds driven by (1) non-uniform forces from the surrounding glass, and (2) mutual interactions between the seeds. At small separations and low misorientation, each seed rotates toward perfect alignment, ultimately forming a single crystal. The onset and rate of alignment, as well as subsequent crystal growth, are strongly dependent on the growth temperature. In contrast, at larger separations and higher misorientation, the seeds cannot achieve full alignment before coalescing, resulting in polycrystalline structures.

1. Introduction

Ever since its accidental discovery by Stookey [1], glass-ceramic materials have evolved as an important class of materials for various applications ranging from kitchen cooktops to dental fillers, and laser glass to ultra-low expansion (ULE) mirrors. The applications of glass-ceramics are wide-ranging because they allow us to infuse unique crystalline properties in an otherwise isotropic, homogeneous glass matrix [1,2]. Industrial-scale manufacturing of all glass-ceramics involves growing crystals inside a glass host by suitably controlling the crystal nucleation and growth conditions [3,4]. This is fundamentally different from the well-known Czochralski process [5] used to produce a high-quality defect-free single crystal. Thermal treatment is most commonly used to manufacture glass-ceramics. It involves heating the glass to a nucleation temperature where large number of nuclei forms, followed by heating further to a growth temperature. During this ceramization process, once stable nuclei form, the rate at which crystals grow depends on the speed with which atoms or molecules diffuse from the surrounding glass to across the interface into the growing crystal [6]. Since multiple crystals grow simultaneously during typical ceramization, any interaction between seeds and impact on the growth of a seed from the presence of nearby seeds are vital to understanding the microstructure of glass-ceramic, which determines its properties.

Although isolated single crystals with laser-induced heating can be formed by adjusting the glass composition, laser scanning speed, and laser power density [7], industrially made glass-ceramics are mostly polycrystalline with large crystalline regions separated by residual glass. The nature of the orientation of neighboring crystal grains and the boundary that separates them is crucial to creating products with polar properties. Glass-ceramics with polar properties (piezoelectricity and ferroelectricity) can be achieved if individual crystallites collectively demonstrate crystallographic and polar orientation during crystallization [8,9]. Oriented crystal growth can be achieved experimentally via kinetic control or thermodynamic control [10,11]. Kinetic control is exploited in surface crystallization while thermodynamic control involves using electric, mechanical, or magnetic fields as driving forces to favor oriented crystallization in the fabrication of glass-ceramics [12,13].

Ferroelectric $LiNbO_3$ glass-ceramics have gained significant research interest owing to their wide applications arising from excellent electromechanical, thermal and dielectric properties [14,15]. These glass-ceramics are formed from glasses with a large fraction of the ferroelectric phase and a low concentration of glass network formers [9]. Experimental fabrication of SiO_2-based glass networks for $LiNbO_3$ glass-ceramics has highlighted a glass-forming region with high silica content [16–18]. On the simulation side, the crystallization of

* Corresponding author.
E-mail addresses: h.jain@lehigh.edu (H. Jain), vod2@lehigh.edu (V. Dierolf).

https://doi.org/10.1016/j.actamat.2026.122453
Received 28 February 2026; Received in revised form 9 June 2026; Accepted 12 June 2026
Available online 19 June 2026

$LiNbO_3$ in lithium niobosilicate glasses ($xLiNbO_3$-(1-x)SiO_2) is highly suppressed even at 5 mol % SiO_2. This limits us to simulate the growth of multiple seeds of $LiNbO_3$ crystal inside $LiNbO_3$ glass. Atomic scale understanding of the growth of one crystal in $LiNbO_3$ [19,20], ZnSe [21], and metallic glasses [22] using molecular dynamics simulation has been previously reported. So far, no attempts have been made to model the growth of crystals using multiple seeds, which is required to explore the influence of one crystal on the growth of its neighbors. Accordingly, in this work, we explore the growth of two seeds as a function of distance and misorientation angle between them.

It has been reported earlier that the glass outside the seed causes non-zero torque on the seed thereby causing the seed to rotate during early stages of growth [23]. Thus, a glass cannot be considered isotropic on the scale of glass-crystal interface. We build on this work to study seeded crystal growth (SCG) with multiple seeds and explore the effect of their misorientation and separation on the likelihood of growing a single crystal from two seeds. In general, it is interesting to determine how the interaction between the seeds may affect their rotation, thus indicating whether the seeds will merge to form a single-crystal or polycrystalline glass-ceramic. For the latter, we would also like to know the nature of the boundary separating the crystal grains and its dependence on the relative misorientation and separation.

2. Methodology and models

We have created models of seeded glass of $LiNbO_3$ with around a half million atoms, containing two seeds, at experimental density using the traditional melt-quench (MQ) technique. The pairwise interaction for this simulation is a combination of a long-range Coulomb term and a short-range Buckingham term, with a partial effective charge. The overall interaction takes the form:

$$V_{ij}\left(r_{ij}\right) = \frac{Z_i Z_j e^2}{4\pi\epsilon_0 r_{ij}} + A_{ij} exp\left(-\frac{r_{ij}}{\rho_{ij}}\right) - \frac{C}{r_{ij}^6} \quad (1)$$

where Z_i and Z_j are the partial charges of atoms i and j, and r_{ij} is the interatomic distance between them. The empirical parameters for the Buckingham potential were taken from Sun et al. [24]. The discrepancy of the Buckingham potential at short interatomic distances has been corrected using a correction factor [25]. Since 15 $\AA$ is larger than the critical nucleus size [20], we chose both seeds placed in the glass to be initially 15 $\AA$ to model crystal growth with multiple seeds. The liquid melt was created, outside the seed, at 6000K and gradually cooled to room temperature with an equilibration cycle between the subsequent cycles of cooling for a total simulation time of 2.15 ns, equivalent to a cooling rate of 2.65 K/ps. Selective dynamics was employed to keep the seeds fixed during the entire MQ cycle, while moving the atoms outside the seeds, in order to generate a seeded glass. All melt-quench and SCG molecular dynamics simulations were performed using the open source LAMMPS package [26]. Misorientation angle measures the relative orientation of the c-axis of the two $LiNbO_3$ crystal seeds, and hence the nomenclature of the investigated configurations is Z-x where 'x' is the misorientation angle (in degrees) between the two seeds. The complete study consists of 16 configurations, four for each of the four seed separation distances. The details of the system are described in Table 1. For example, the geometry of the starting seeds with different misorientations in Configuration II is shown in Fig. 1 (left).

Once the melt-quench cycle is complete, the seeded glass is subjected to a crystal growth simulation. The seeded glass structure is passed on to an NPT ensemble (3000 K, 1 atm) allowing for atomic dynamics of all atoms present in seeded crystal and glass. The time evolutions of the crystal seed that grows and the residual glass have been tracked using a machine-learning clustering algorithm based on static and dynamic structural factors [20]. Visualizations have been created using the 3D visualization software OVITO [27]. Configuration I which had seeds separated by 45 $\AA$ appeared to have a very thin glass layer that separated them after the MQ cycle and hence is not included in further analysis.

Table 1
Details of models of seeded glass generated using melt-quench for SCG simulation.

	Seed radius	Models	Seed separation
Configuration I	15 Å, 15 Å	Z-0, Z-10, Z-30, Z-60	45 Å
Configuration II	15 Å, 15 Å	Z-0, Z-10, Z-30, Z-60	55 Å
Configuration III	15 Å, 15 Å	Z-0, Z-10, Z-30, Z-60	60 Å
Configuration IV	15 Å, 15 Å	Z-0, Z-10, Z-30, Z-60	65 Å

We developed a technique to quantify crystal rotation observed during SCG. The algorithm for calculating the rotation angle during SCG is as follows:

- select a plane of Nb atoms, one in each seed, as shown in Fig. 1 (left) before the SCG starts
- determine a best-fitted plane using least square fit for each set of atoms in an atomic plane
- find angle between these fitted planes at each snapshot

A similar mathematical algorithm was previously reported to calculate the rotation of magnetic microdisks under the effect of the magnetic field [28].

3. Results and discussion

3.1. Structure of seeded glass

The final structure obtained after the melt-quench cycle had two seeds surrounded by a glassy arrangement of atoms across all misorientations and seed separation. The radial distribution function for the seeded glass systems in Configuration II, shown in Fig. 1 (right), for the glass outside the seeds revealed a minimal qualitative difference. This result suggests similar metal–oxygen (first peak), oxygen–oxygen (second peak) and other possible atomic environments across all the configurations. Such findings confirm the reliability of the potential used in the simulation, the melt-quench algorithm employed and confirm the uniformity of the glass outside the seeds in terms of structural correlations. Similar conclusions were drawn from the analysis of models in Configuration III and IV.

3.2. Growth rate in SCG with multiple seeds

The quantification of the crystallinity of the system during SCG is tracked with the evolution of the fraction of crystal-like atoms. The prediction of whether an atom is crystal-like or glass-like is made using a machine-learned clustering algorithm based on static structural features (Steinhardt parameter [29], number of connections [30]) as well as temperature dynamics of the atoms [20]. The time evolution of the crystal fraction for various models is shown in Fig. 2. The crystal growth rates for different seed separations and relative misorientations are comparable to each other. However, the temperature dependence of the growth rate, shown in Fig. 3, suggests that it is maximum for annealing at 3000 K, which is below the melting temperature of 3300 K [20]. Although higher than the experimental value, the observation of a peak crystallization temperature below the melting but above the glass transition temperature is analogous to experimental observations of crystal growth [31]. This temperature of 3000 K supplies sufficient atomic mobility to the heavier Nb atoms to facilitate crystallization while avoiding the full disorder of the melt. However, at lower temperatures, the Nb atoms tend to slow down considerably and reduce the crystallization rate. These findings suggest that the rate of addition of atoms to the growing seed has a strong dependence on the temperature.

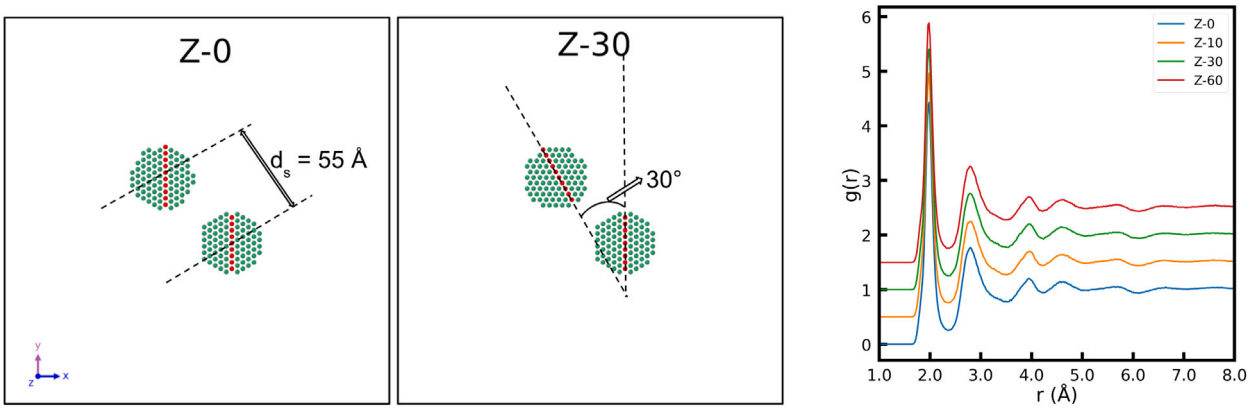

Fig. 1. (left) Initial configuration of the seeds, both 15 $\mathring{A}$, before the melt-quench. (right) Radial distribution function for the glass after melt-quench cycle.

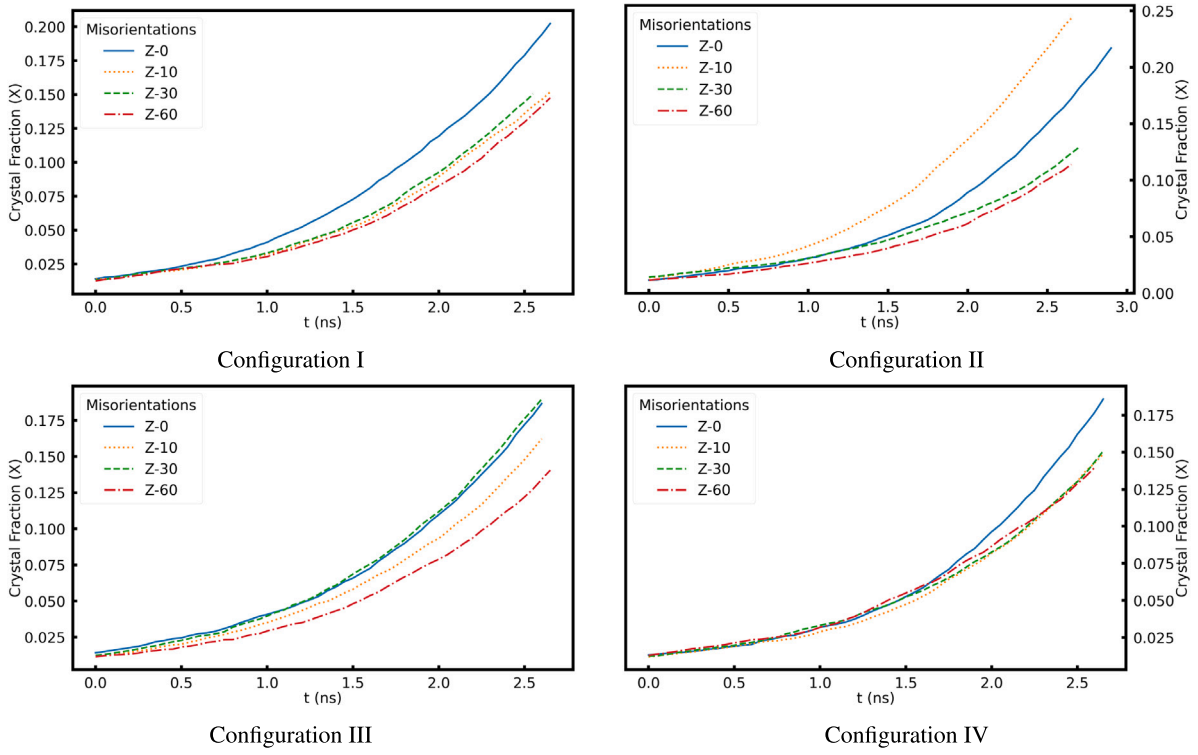

Fig. 2. Time evolution of the crystal fraction (X) during SCG with varying seed separation (Configurations I vs. II vs. III vs. IV) and misorientation angles (plots within any one panel).

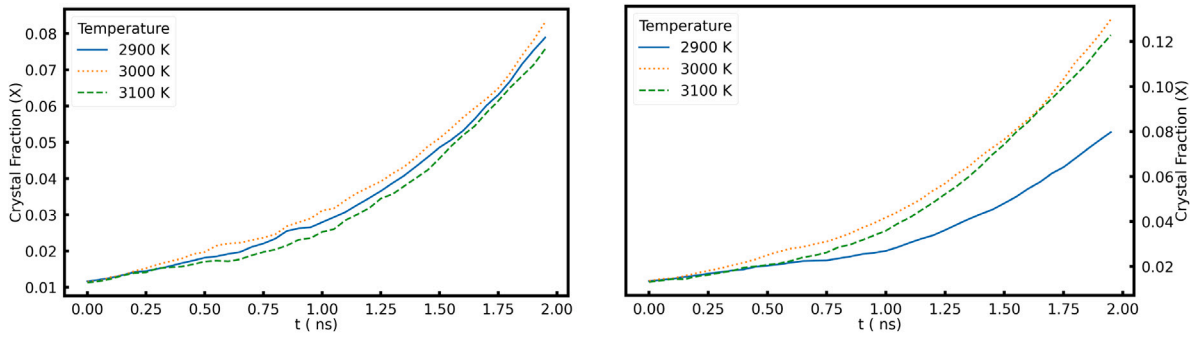

Fig. 3. Time evolution of the crystal fraction (X) during SCG at three different annealing temperatures for Configuration II Z-0 (left) and Configuration II Z-10 (right).

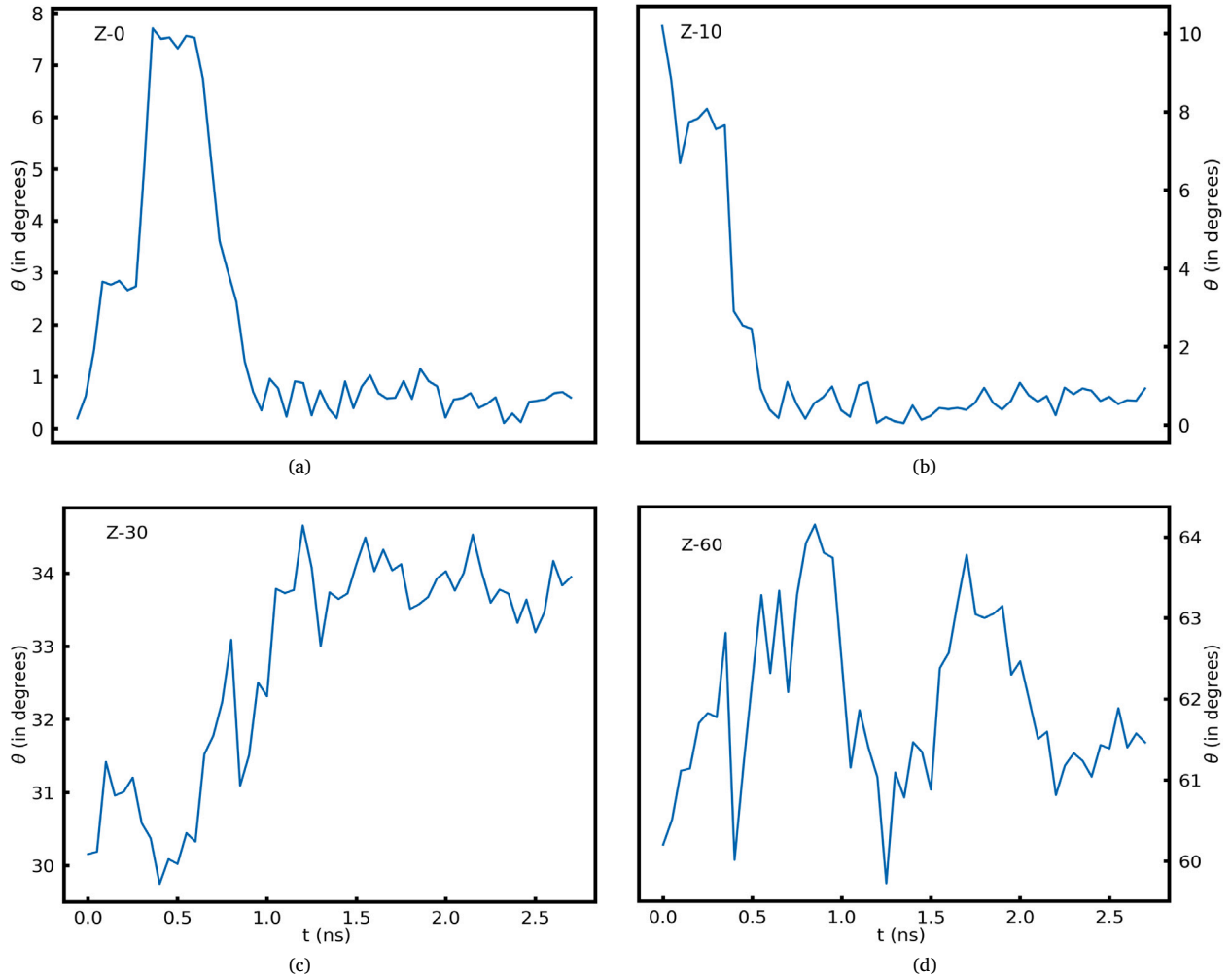

Fig. 4. Time evolution of the angle between seeds in Configuration II during SCG for different misorientation angles.

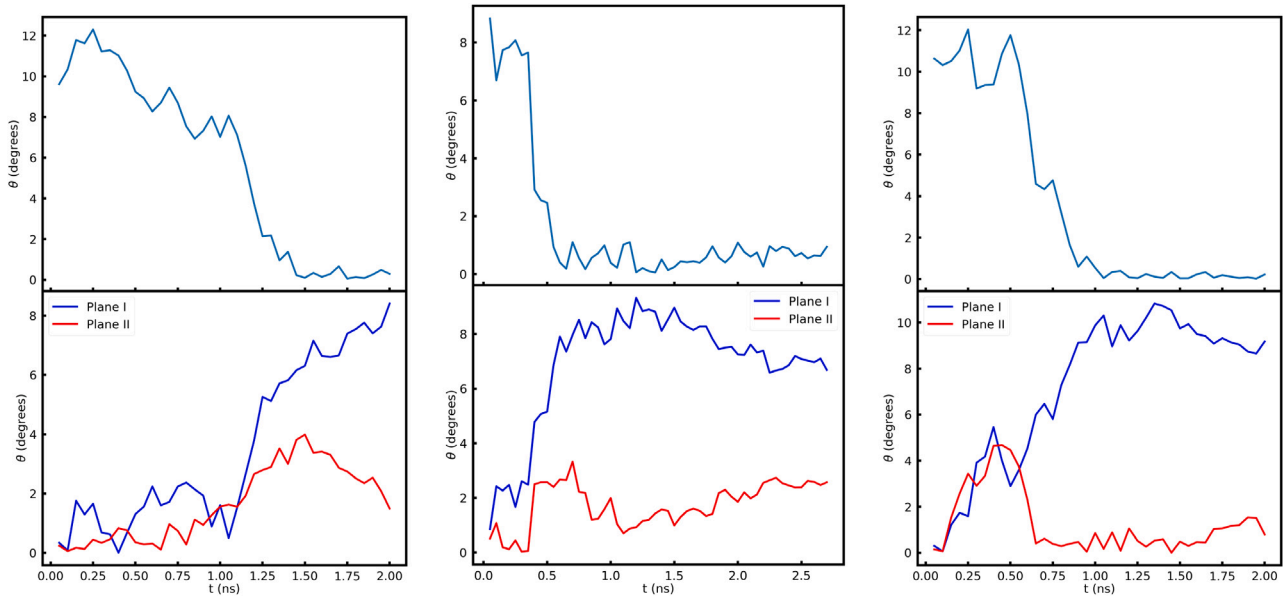

Fig. 5. Time evolution of the angle between seeds (top) and the individual seed rotation (bottom) during SCG at 2900 K (left), 3000 K(middle), and 3100 K (right) for Configuration II Z-10. Plane I and II are representative planes in the crystal seed I and II respectively, colored red in Fig. 1(left).

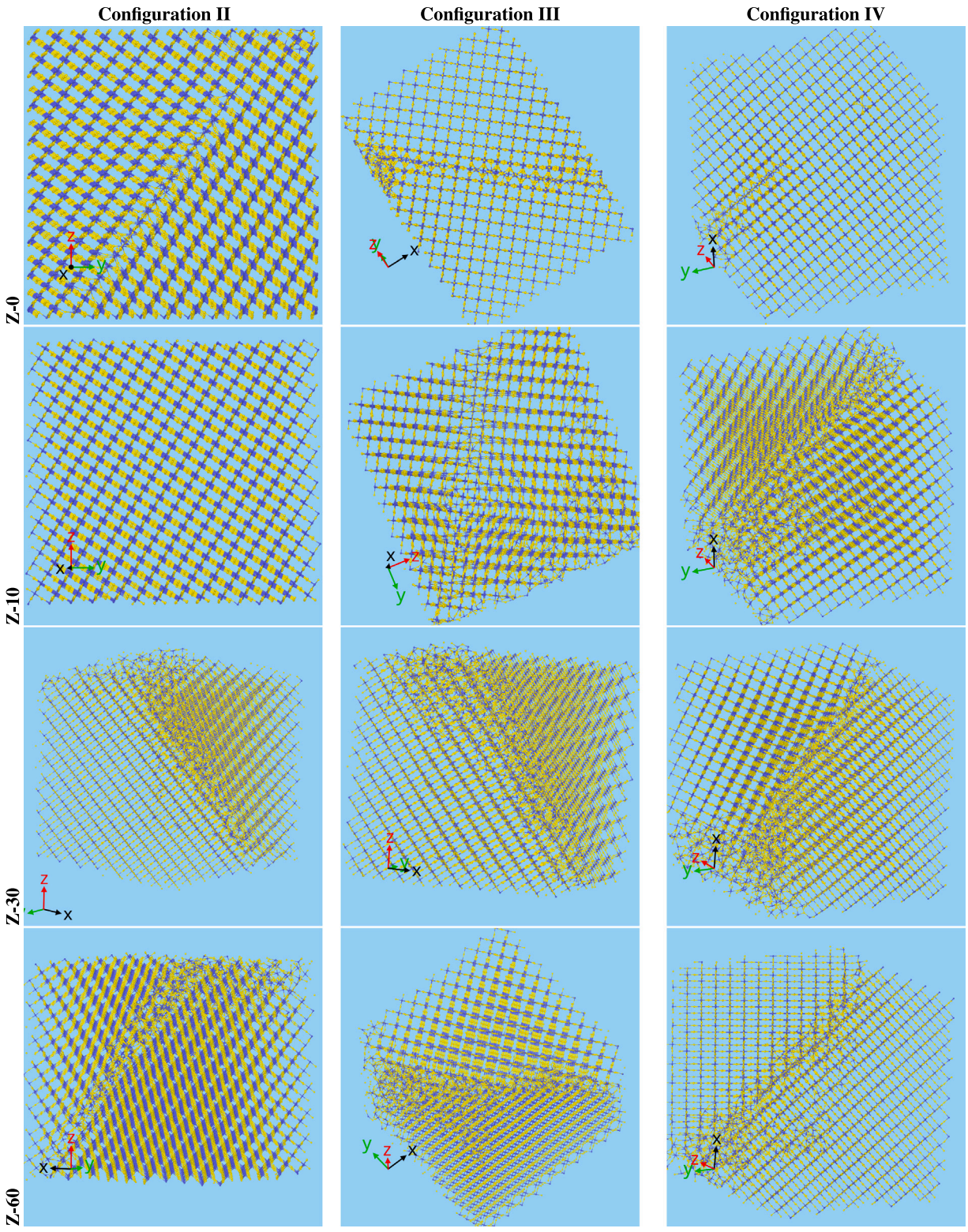

Fig. 6. Structure of the crystallized region after SCG with two seeds with different initial misorientations (across the column) and seed separations (across the rows).

3.3. Rotation of seeds during SCG

Each crystal seed rotates during early stages of crystal growth due to non-zero force/torque from the glass outside the seed as reported earlier for systems with a single seed [23]. Two seeds present in the glass matrix in this study also showed rotations during SCG for all seed separation and misorientation angle combinations. A representative example of the time evolution of the angle of misorientation between seeds for Configuration II models is shown in Fig. 4. It can be seen in Fig. 4(a) that perfectly oriented crystal seeds (Z-0) that move out of alignment (almost 8°) during the early stages of crystal growth move back to perfect alignment. This observation suggests a strong

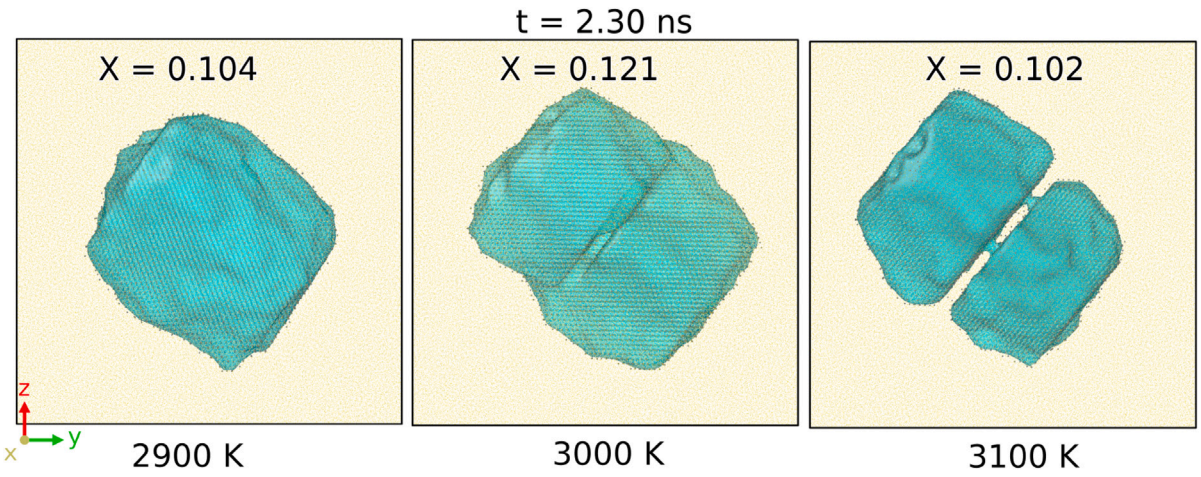

Fig. 7. Crystals grown starting from Configuration II Z-0 under SCG at different temperatures.

interaction between the seeds aided by a strong proclivity to move to energetically favorable perfect alignment and a growth afterward as a single crystal. A move from an initial 10° misorientation to a perfect orientation and then a single-crystal growth in Configuration II and III suggest a strong coupling between two seeds and a proclivity to perfect alignment. A visualization of the rotation towards perfect alignment is shown in the movie here. However, for larger misorientations (> 10°), the seeds that grow during SCG cannot align perfectly before they touch each other and thus cannot grow as a single crystal. In other words, the rate of alignment is faster than the growth rate for lower misorientation while the opposite is true for higher degrees of misorientation. A similarity across all misorientations is that the seeds tend to stop rotating after a certain time after the crystal becomes too large for the force originating from the glass to rotate them.

The temperature dependence of rotation has been studied for Configuration II Z-10 model by comparing the time evolution of rotation at different temperatures (2900 K, 3000 K, 3100 K). The evolution of the angle of misorientation between the seeds, shown in Fig. 5 (top), suggests that the transition from a 10° misorientation to a perfect orientation during SCG is observed at all temperatures, although the time to achieve perfect orientation varies, as does the crystal growth rate (shown in Fig. 3(right)). Also, Fig. 5 (bottom) shows that each seed rotates on its own but the coupling present due to the proximity pulls them towards perfect orientation. This observation indicates a strong coupling between the seeds misoriented by small angles, which ultimately pushes them back into perfect orientation.

3.4. Nature of the crystal assembly

The nature of the combined crystal assembly grown from two seeds depends directly upon the rotation the seeds go through during the growth before their surfaces meet each other. SCG with multiple seeds shows crystal growth is coupled with the rotation of individual seeds for all seed separation and misorientations. The crystal assembly may be characterized by whether the final result is a single crystal or polycrystalline ceramic. The crystallized regions in systems with varying initial misorientation and seed separation are shown in Fig. 6. The structure of these regions suggests that perfect initial orientations (Z-0) result in perfectly aligned grains even for higher separation. However, there is often a narrow residual glass region between the seeds (as seen in Z-0 models in all separations). This could arise if the atoms in the boundary cannot align themselves fast enough with the growing seeds that engulf the region between the seeds. In other words, even though the grains have a high proclivity to align perfectly, the atoms in the residual glass that separate them cannot orient and align fully with the growing crystals. The overall crystal, as seen in a Configuration II Z-0, will have perfectly oriented grains but a very narrow region that is not perfectly aligned to become one single crystal. Lowering the crystallization rate by reducing the SCG temperature allows more time for the residual glass to align perfectly to the growing crystal thereby creating a perfect single crystal as seen in Fig. 7.

At low misorientations Z-10, the interaction between seeds is strong enough to achieve their perfect alignment during SCG, provided the seeds are not too far (Configuration II, Configuration III). However, at larger separation (Configuration IV), the seeds tend to grow as individual grains without transitioning towards a perfect orientation, thereby resulting in a thick residual glass layer separating them.

At higher misorientations (Z-30, Z-60), the seeds grow as independent grains and cannot reorient themselves to align perfectly at all seed separations. These configurations rule out the possibility of creating a single crystal because the grains are misoriented and are separated by a residual glass layer when they meet during the growth process. To provide a visualization of the growth of the seeds and grain alignment for various misorientations in Configuration II and III, movies have been added here and here. As a cross-validation check, we performed crystal growth simulations with varying structure of the matrix around the two seeds, such as by using a longer melt-quench, for Batch II Z-O and Z-10 configuration. There was no effect of such variation of the glass structure on the alignment of two seeds; the two seeds aligned perfectly as before.

While the simulations demonstrate that mutual seed rotation can occur, the weak distance dependence suggests that this interaction is subtle and may only become apparent under conditions of reduced noise and enhanced structural coherence, such as those present in the model system used in this work.

4. Conclusion

We investigated the dynamics of crystal growth of two seeds in a glass using large-scale atomic simulations containing half a million atoms. We explored how seed positioning and crystallographic misorientation influence crystal formation inside glass. The research revealed several key insights:

1. The crystal growth rate exhibited remarkable consistency, showing minimal sensitivity to misorientation angles and seed distances when the seeds were sufficiently separated.
2. Across all simulation scenarios, we consistently observed crystal rotation during the early stages of growth, indicating dynamic structural reorganization. Seeds exhibited individual rotation but it was driven towards some desired orientation if there was a seed with low misorientation in close proximity.

3. Optimum conditions for a perfect alignment of the grains were determined by observing the crystallization of the seeds at various initial misorientations. The final crystalline structure, whether it developed as a single crystal or remained polycrystalline, was critically dependent on both the initial misorientation between the seeds and their spatial separation.
4. There was a temperature (3000 K) at which the growth rate was maximum, as predicted by classical theory.
5. Whether two seeds grew to become a single crystal or polycrystals depended not only on their separation and misorientation but also on the temperature. A temperature lower than the peak growth temperature exhibited greater proclivity to form a single crystal.

In summary, the present study has provided a comprehensive understanding of the complex mechanisms that govern crystal growth from multiple seeds and the intricate relationships between initial seed conditions, temperature, and the resulting crystalline structures.

CRediT authorship contribution statement

R. Thapa: Writing – review & editing, Writing – original draft, Visualization, Validation, Software, Methodology, Investigation, Formal analysis, Data curation, Conceptualization. **H. Jain:** Supervision, Methodology, Funding acquisition, Conceptualization. **V. Dierolf:** Validation, Supervision, Resources, Funding acquisition, Conceptualization. **M.E. McKenzie:** Writing – review & editing, Writing – original draft, Validation, Formal analysis, Conceptualization.

Declaration of competing interest

The authors declare that they have no known competing financial interests or personal relationships that could have appeared to influence the work reported in this paper.

Acknowledgments

This work was supported by the US Department of Energy (DoE), Office of Science, Basic Energy Sciences, under award DE-SC0005010. Computer simulations were performed using ACCESS [32] at Pittsburgh Supercomputing Center through mat230020p allocation from the Advanced Cyberinfrastructure Coordination Ecosystem: Services & Support (ACCESS) program, which is supported by the National Science Foundation, United States grants 2138259, 2138286, 2138307, 2137603, and 2138296. We also acknowledge the computing resources available through Lehigh Supercomputer center to perform some of our simulations.

References

[1] S.D. Stookey, Method of making ceramics and product thereof. 2920971, 1956.
[2] A. Sakamoto, S. Yamamoto, Glass–ceramics: Engineering principles and applications, International Journal of Applied Glass Science 1 (3) (2010) 237–247.
[3] J. Deubener, M. Allix, M. Davis, A. Duran, T. Höche, T. Honma, T. Komatsu, S. Krüger, I. Mitra, R. Müller, S. Nakane, M. Pascual, J. Schmelzer, E. Zanotto, S. Zhou, Updated definition of glass-ceramics, JNonCrystSolids 501 (2018) 3–10, 12th International Symposium on Crystallization in Glasses and Liquids.
[4] L. Fu, H. Engqvist, W. Xia, Glass–ceramics in dentistry: A review, Materials 13 (5) (2020).
[5] J. Czochralski, A new method for measuring the crystallization rate of metals, ZPhysChem 92 (1918) 219.
[6] A.K. Varshneya, J.C. Mauro, Chapter 3 - glass formation principles, in: Fundamentals of Inorganic Glasses (Third Edition), third ed., Elsevier, 2019, pp. 37–69.
[7] K. Veenhuizen, D. Nolan, B. Aitken, V. Dierolf, H. Jain, Fabrication of graded index single crystal in glass, Scientific Reports 7 (2017) 44327.
[8] A. Halliyal, A. Safari, A.S. Bhalla, R.E. Newham, L.E. Cross, Grain-oriented glass-ceramics for piezoelectric devices, JAmCeramSoc 67 (5) (1984) 331–335.
[9] K. Gerace, J. Mauro, C. Randall, Piezoelectric glass–ceramics: Crystal chemistry, orientation mechanisms, and emerging applications, JAmCeramSoc 104 (2021).
[10] C. Rüssel, Oriented crystallization of glass. a review, JNonCrystSolids 219 (1997) 212–218, Glass Crystallization.
[11] W. Wisniewski, K. Thieme, C. Rüssel, Fresnoite glass-ceramics– a review, ProgMaterSci 98 (2018) 68–107.
[12] Y. Ochi, T. Meguro, K. Kakegawa, Orientated crystallization of fresnoite glass-ceramics by using a thermal gradient, JEurCeramSoc 26 (4) (2006) 627–630, Proceedings of the International Symposium on Inorganic and Environmental Materials, Eindhoven, NL, October 2004.
[13] H.C. Wang, Q.M. Liu, J.S. Cheng, Field-assisted isothermal oriented crystallization of SrO-TiO_2-SiO_2 polar glass-ceramics, in: Advanced Synthesis and Processing Technology for Materials, in: Advanced Materials Research, vol. 66, Trans Tech Publications Ltd, 2009, pp. 49–52.
[14] R.S. Weis, T.K. Gaylord, Lithium niobate: Summary of physical properties and crystal structure, Applied Physics A 37 (4) (1985) 191–203.
[15] G. Fernandes, P. Manuel, M.A. Valente, Ferroelectric glass-ceramics, MRSBull 42 (3) (2017) 213–219.
[16] M. Todorović, L. Radonjić, pCeramInt 23 (1) (1997) 55–60.
[17] E. Prasad, M. Sayer, H. Vyas, Li+ conductivity in lithium niobate: silica glasses, JNonCrystSolids 40 (1) (1980) 119–134.
[18] N.S. Prasad, K.B.R. Varma, Crystallization kinetics of the $LiBO_2$ – –Nb_2O_5 glass using differential thermal analysis, JAmCeramSoc 88 (2) (2005) 357–361.
[19] W. Sun, V. Dierolf, H. Jain, Molecular dynamics simulation of seeded crystal growth in glass, Journal of Non-Crystalline Solids: X 15 (2022) 100113.
[20] R. Thapa, M.E. McKenzie, E. Mustermann, J. Kaman, V. Dierolf, H. Jain, Machine learning based insights of seeded congruent crystal growth of $LiNbO_3$ in glass, ActaMater 276 (2024) 120115.
[21] L. Separdar, J.P. Rino, E.D. Zanotto, Decoding crystal growth kinetics and structural evolution in supercooled ZnSe by molecular dynamics simulation, ComputMaterSci 212 (2022) 111598.
[22] F. Chen, Z. Nussinov, K.F. Kelton, Crystal nucleation and growth in liquids: Cooperative atom attachment and detachment, PhysRevB 108 (2023) 064205.
[23] R. Thapa, E.J. Musterman, H. Jain, V. Dierolf, M.E. McKenzie, Rotation of crystal seed during early stages of growth reveals the anisotropy of glass matrix, Advanced Science 13 (29) (2026) e16671.
[24] W. Sun, K. Veenhuizen, J. Marsh, V. Dierolf, H. Jain, ComputMaterSci 207 (2022) 111307.
[25] L. Deng, J. Du, JAmCeramSoc 102 (5) (2019) 2482–2505.
[26] A.P. Thompson, H.M. Aktulga, R. Berger, D.S. Bolintineanu, W.M. Brown, P.S. Crozier, P.J. in 't Veld, A. Kohlmeyer, S.G. Moore, T.D. Nguyen, R. Shan, M.J. Stevens, J. Tranchida, C. Trott, S.J. Plimpton, LAMMPS - a flexible simulation tool for particle-based materials modeling at the atomic, meso, and continuum scales, ComputPhysComm 271 (2022) 108171.
[27] A. Stukowski, Visualization and analysis of atomistic simulation data with ovito–the open visualization tool, ModellingSimulMaterSciEng 18 (1) (2009) 015012.
[28] C. Liu, J. Cai, D. Gong, W. Zhang, D. Zhang, Fabrication and uniform alignment of nickel-coated diatomite flakes by rotating magnetic fields, JMagnMagnMater 484 (2019) 472–477.
[29] P.J. Steinhardt, D.R. Nelson, M. Ronchetti, Bond-orientational order in liquids and glasses, PhysRevB 28 (1983) 784–805.
[30] P. Rein ten Wolde, M.J. Ruiz-Montero, D. Frenkel, Numerical calculation of the rate of crystal nucleation in a Lennard–Jones system at moderate undercooling, JChemPhys 104 (24) (1996) 9932–9947.
[31] K. Veenhuizen, C. Barker, J. Franklin, S. McAnany, B. Aitken, D. Nolan, V. Dierolf, H. Jain, The role of glass composition in the 3D laser fabrication of lithium niobate single crystal in lithium niobosilicate glass, OptMater 128 (2022) 112380.
[32] T.J. Boerner, S. Deems, T.R. Furlani, S.L. Knuth, J. Towns, ACCESS: Advancing innovation: NSF's advanced cyberinfrastructure coordination ecosystem: Services & support, in: Practice and Experience in Advanced Research Computing, PEARC '23, Association for Computing Machinery, New York, NY, USA, 2023, pp. 173–176.